Voltage selection of physisorbed or chemisorbed 4-cyanobenzoate on a nanostructured silver electrode and the dual electronic structure of charged metal-molecule hybrids

Samuel Valdivia [a], *Francisco José Avila* [a], *Juan Carlos Otero* [a]*, *Isabel López-Tocón* [a]*

[a] Andalucía Tech, Unidad Asociada CSIC, Departamento de Química Física, Facultad de Ciencias, Universidad de Málaga, Málaga, Spain.

* Corresponding author. E-mail address: tocon@uma.es (I. López-Tocón); jc_otero@uma.es (J.C. Otero)

Declaration of interest: none

Abstract

Applied electric potentials tune SERS wavenumbers due to vibrational Stark effect, but some modes of $4CNB^-$ show two differentiated regions, being redshifted at more negative potentials than the potential of zero charge of the electrode but remain unshifted at positive potentials. DFT calculations have been carried out for a model where $4CNB^-$ is linked through the carboxylate $[Ag_n^q\text{-}OOC(4CNB^-)]^{q-1}$ or the nitrile $[Ag_n^q\text{-}NC(4CNB^-)]^{q-1}$ to stick-like silver clusters $[Ag_n]^q$ with different densities of charge (q_{eff} =q/n). The comparison between calculated and experimental wavenumber shifts points out that $4CNB^-$ is always adsorbed through the carboxylate. The dual behaviour of the wavenumbers is due to the existence of two types of electronic structure of the metal-molecule hybrid. Physisorbed (P-hybrid, repulsive) or chemisorbed (C-hybrid, attractive) surface complexes are selected by the sign of the surface excess of charge of the electrode. The electronic structure of weakly bonded P-hybrid is very sensitive to the voltage and their wavenumbers are continuously shifted, while the wavenumbers of the strong C-hybrid remain almost unshifted. This result proves the dual nature of the electronic structure of molecules bonded to charged metal electrodes or nanoparticles which can be responsible of the qualitative changes observed in electrochemical or molecular electronics experiments.

Keywords: Nanostructured electrode, SERS spectroscopy, DFT calculations, 4-cyanobenzoate, Vibrational Stark effect.

1. Introduction

Surface-Enhanced Raman Scattering (SERS) [1] is a very powerful spectroscopic technique for detecting pollutants or molecules [2,3], even with poor solubility in water [4], at trace level concentration due to the enormous enhancement of Raman signal when the systems are located close to a nanostructured metal surface of coinage metals. SERS is also very useful for studying metal-molecule interfacial phenomena involved in electrochemistry, heterogeneous adsorption, catalysis or in corrosion processes [5,6], where all the properties of the surface complex are determined by its electronic structure which is controlled by applied electric potentials. SERS features, such as changes in the relative intensities and wavenumbers as well as the broadening of the vibrational bands upon adsorption, provide invaluable information at molecular level on the chemical species adsorbed, the interacting functional group with the metal [7-11] or for monitoring surface reactions [5,12].

Much attention has been paid to adsorption studies of para-substituted benzonitriles on different silver surfaces by using SERS and other vibrational spectroscopies [7,13-18]. 4-cyanobenzoic acid (4CNBH) [7,13-15] is an interesting system because it is able to interact with the metal through two functional groups with electron-withdrawing (nitrile group) and electron-donating (carboxylate group) character. Moreover, nitrile can be bonded to the surface via σ donation from the electron lone pair of the nitrogen or via π donation, companied by π^* backdonation from the CN triple bond. Both kind of bonding would result in blue and red wavenumber shifts of the very characteristic CN stretching band, respectively, as it has been observed in organometallic compounds [19,20]. These two possibilities would give end-on (perpendicular) and side-on (parallel) surface orientations, respectively. As a result, contradictory conclusions about the surface orientation of adsorbates have been reported even in the case of the simple cyanide anion [21]. For instance, blue-shifts of the CN stretching band in some benzonitrile derivatives like (methylthio)benzonitrile [12] have been explained on the basis of a flat orientation via both the sulphur atom and the nitrile group, being in contradiction with the expected behaviour for a π−complex.

Organic acids like 4CNBH absorbs ionized ($4CNB^-$) on nanostructured silver surfaces [7,13-15] but, depending on different factors such as the nature of the metal substrate (colloidal solutions [7,13], films, powders [13-15]) or other experimental conditions like the polarity of the solvent [15], $4CNB^-$ can be bonded with perpendicular orientation through one of the two functional groups or lying flat, so that carboxylate and nitrile groups and the aromatic ring can interact with the surface [13-15,22,23].

Many published SERS works have been focussed on the effect of the analysis of vibrational features such as the broadening of the CN stretching band and the wavenumber shifts upon adsorption. Scarce theoretical studies modelling the metal-$4CNB^-$ surface complex have been performed. Only Perry et al. reported DFT calculations where a single silver ion located close to each of the two groups [15].

In this work, electrochemical SERS spectra of $4CNB^-$ have been recorded on a roughened silver electrode at different electrode potentials ranging from 0.0 V to -1.0 V. Electrochemical experiments allow for monitoring the effect of the electrode potential in tuning the vibrational wavenumbers, which is usually called vibrational Stark effect [24]. Experimental vibrational wavenumbers have been correlated to those calculated from a theoretical model of $4CNB^-$ adsorbed on a charged silver surface, shedding light on the preferred adsorption geometry and on the expected wavenumber shifts. In a recent study [25], two different theoretical methodologies to simulate the effect of the electrode potential in the properties of the surface complex have been compared by using metal clusters with different densities of charge or, alternatively, by applying external electric fields. It was concluded that external fields are unable to account for the experimental shifts while the methodology of simulating the applied voltage through $[Ag_n]^q$ metal clusters with different densities of charge reproduces satisfactorily the experimental vibrational shifts of pyridine [25]. This last strategy has been applied to discuss the adsorption of $4CNB^-$ on silver electrode on the basis of DFT calculations. The results shed light on the controversy regarding the functional group that is responsible of the adsorption and confirm, for the first time, the dual behaviour shown by the shifts of the SERS wavenumbers of a polyatomic molecule under applied potentials already observed in the case of the diatomic cyanide ion [21].

2. Material and methods

2.1 Experimental Section

4-cyanobenzoic acid (4CNBH) was purchased from Aldrich chemicals (USA) and used without further purification. Electrochemical SERS experiments were recorded using a non-commercial three electrode cell with a platinum counter electrode, an Ag/AgCl/KCl (sat) reference electrode and a pure silver working electrode, which was firstly polished with 0.30 and 0.05 μm alumina (Büehler, USA) and then electrochemically activated to obtain the required nanostructured surface for strong Raman enhancement. SERS surface activation was made using a 0.1 M Na_2SO_4 aqueous solution as electrolyte by keeping the electrode potential at -0.5 V and then subjecting it to seven 2 s pulses at +0.6 V. A potentiostat model 600E (CH

Instruments Inc., USA) was used to control the electrode potentials. All aqueous solutions were prepared using purified water supplied by a Milli-Q system (resistivity over 18 MΩcm). In order to avoid aggregation or the formation of dimmers as it occurs in most benzoic acids, a concentration of 10^{-2} M/0.1 M aqueous solution of 4CNBH/Na_2SO_4 at basic medium, pH=12, was used to record SERS spectra from 0.0 V up to -1.0 V by step of -0.1 V. A single scan and 10 s exposure time were selected to avoid sample damage. The sequence of spectroelectrochemical series of spectra was recorded several times showing good reproducibility.

Raman spectrum of a 0.5 M aqueous solution of the acid at pH=12 ($4CNB^-$) and SERS spectra were recorded by using a Renishaw InVia Qontor micro-Raman spectrometer (Renishaw, UK) with 1 cm^{-1} spectral resolution under 785 nm excitation. No evidence of electrochemical reduction of the nitrile group has found at negative potentials contrary to what happen in related aromatic nitriles [5,6]. An adapted objective (f:30 mm) to work in macro conditions was used in spectroelectrochemical experiments. The laser power at the sample was 5 mW and Wire 2.0 software (Renishaw) was used for spectral acquisition and manipulation.

2.2 Theoretical model and DFT calculations

The effect of the electrode potential has been simulated in theoretical calculations by using linear metal-molecule complexes of $4CNB^-$ bonded to a terminal silver atom of closed shell stick-like $[Ag_n]^q$ clusters with different sizes (n=3, 5, 7, 8) and charges (q = 0 for n = 8 and q = ±1 for odd n). In this way, the effective density of charge of the cluster is defined as $q_{eff}=q/n$ which ranges from -0.33 to +0.33 a.u. in the series of complexes. It has been previously demonstrated that this range of $\Delta q_{eff} \approx 0.66$ a.u. corresponds quite well with the here discussed range of electrode potentials $\Delta V \approx 1$ V [21,25,26].

Two different types of these bidentate chelating complexes have been considered, $[Ag_n^q\text{-}OOC(4CNB^-)]^{q-1}$ and $[Ag_n^q\text{-}NC(4CNB^-)]^{q-1}$, given that $4CNB^-$ is a bifunctional system able to be linked to the metal surface through carboxylate or nitrile groups [11,27]. Figure 1 shows the supermolecule models used in simulating the effect of the electrode potential on the molecular electronic structure of the surface complex. All the geometrical structures of isolated $4CNB^-$, $[Ag_n]^q$ clusters and their complexes were optimized for the respective lowest singlet states under C_{2v} symmetry. Standard spin-unpolarized Density Functional Theory (DFT) calculations as implemented in the Gaussian09 suit of programs [28] have been carried out for geometry optimizations and calculations of the corresponding harmonic vibrational

wavenumbers. B3LYP [29,30] and M06-HF [31] functionals were employed with the LanL2DZ basis set [32-34]. Although the long-range corrected M06-HF functional overestimates the computed vibrational wavenumbers in comparison with those calculated with B3LYP, it has been selected in order to compare the results with those previously published which were focussed on metal-molecule charge transfer processes [35]. Other functionals or larger basis sets do not improve the accuracy of the theoretical predictions concerning vibrational wavenumber shifts as it has been demonstrated in a previous work [25].

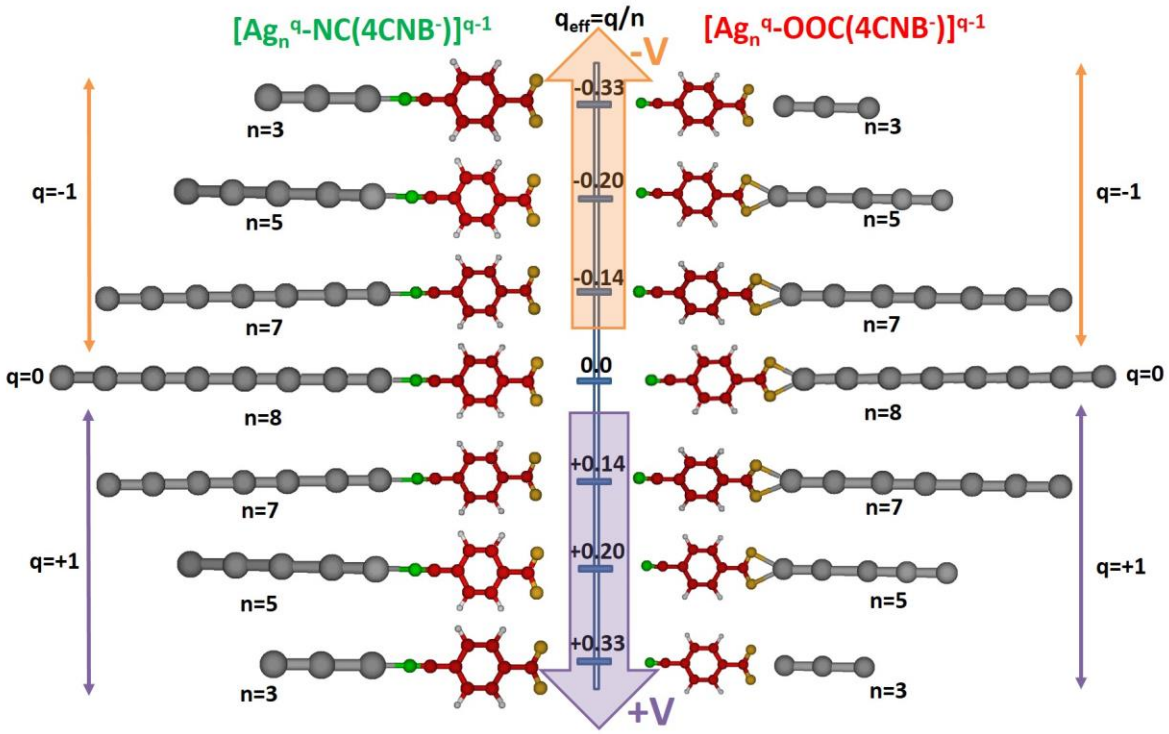

Figure 1. Supermolecules simulating the effect of the density of charge (q_{eff}=q/n) of the silver clusters on the electronic structure of Ag_n^q-4CNB$^-$ complexes bonded through the cyanide or the carboxylate.

C_{2v} geometrical parameters of isolated 4CNB$^-$ agrees quite well with the crystallographic data [36] (Table S1) and reproduces the shortening of the central C-C bond of the benzene ring which is a common feature in para-substituted benzonitriles [37-40] due to the cooperative interaction between the electron-withdrawing and electron-donating character of the two substituents as it happens in para-substituted nitrobenzenes [39]. Crystallographic data of neutral 4CNBH acid point out that the aromatic ring is slightly distorted from planarity, ca. 0.008 Å, and that the carboxylic group is rotated 7.7º through the exocyclic C-C bond, while

the optimized DFT structure of this neutral species would show a planar C_s structure [41] with similar bond lengths and angles than those of $4CNB^-$ summarized in Table S1.

3. Results and discussion

3.1 Assignment of the Raman and Electrochemical SERS Spectra of $4CNB^-$

Figure S1 shows the Raman spectra of solid 4CNBH and of its aqueous solution in basic medium ($4CNB^-$). The potential-dependent SERS spectra of $4CNB^-$ adsorbed on a roughened silver electrode can be seen in Figure 2. The corresponding assignment of the Raman and SERS bands is broadly in line with the previous reported [7,13,14] and has been performed from DFT normal mode calculations (Table S2) visualized with the MOLDEN program [42]. The main SERS bands correlated well with those observed in the Raman of the aqueous solution and the main lines correspond to totally symmetric A_1 in-plane vibrations (Table S2). Characteristic totally symmetric bands are recorded at about 1610, 1191, 848 and 762 cm^{-1} being assigned as 8a;ν_{ring}, 9a;δ(CH), 1;ν_{ring} and 12;δ_{ring}, respectively, according to the systematic behaviour of the vibrations of para-disubstituted benzene derivatives [43]. Two non-totally symmetric B_2 modes are observed in the Raman spectra of the aqueous solution at 644 and 1416 cm^{-1} and assigned to 6b and 19b fundamentals, respectively. The latter appears as a shoulder of the 1388 cm^{-1} band in the spectrum of the solution and could correspond to the weak band recorded in solid at 1406 cm^{-1}. Finally, the out-of-plane ring-torsional Wilson´s mode 4;τ_{ring},B_1 recorded at 405 cm^{-1} is the only non-totally symmetric vibration recorded in SERS [43]. Only the SERS recorded at -1.0 V seems to show some weak bands which could correspond to decomposition products [6], but the lines of the remaining SERS spectra correlate well with the $4CNB^-$ normal modes.

Regarding the two functional groups, the very characteristic Raman band at about 2230 cm^{-1} is assigned to the CN bond stretching, ν(CN). It is the second most intense band in the Raman spectrum of the solution but becomes very weak in SERS. The strong relative de-enhancement of this SERS band was already observed in the SERS of cyanopyridines [11] and was tentatively explained on the relative orientation of the CN bond with respect to the silver surface, depending on the substitution position of the nitrile [7,44,45], or to the formation of the corresponding amide derivative [46]. This latter possibility has been discarded in our SERS given that no bands related to the amide group have been detected. According to the very popular surface propensity rules derived from the electromagnetic enhancement mechanism of SERS [47,48] the very weak intensity of the ν(CN) band in SERS

should be due to a parallel orientation of the C-N bond with respect to the metal surface, but no main SERS bands assigned to out-of-plane modes are recorded. Moreover, the observed wavenumber shifts due to the adsorption are only consistent with a perpendicular orientation of $4CNB^-$ in the whole range of electrode potentials.

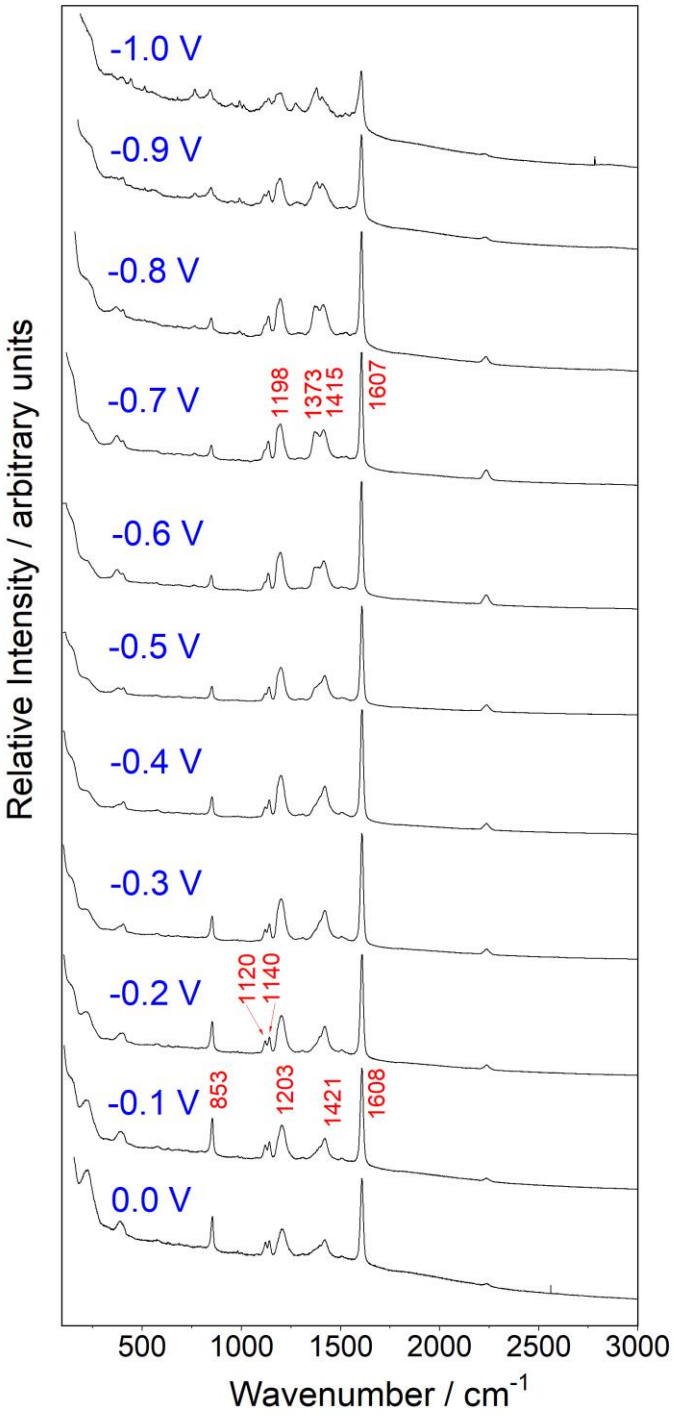

Figure 2. SERS spectra of 10^{-2} M/0.1 M solution of $4CNB^-/Na_2SO_4$ at pH=12 recorded at different electrode potentials using the 785 nm exciting line.

Concerning the carboxylate group, the Raman of the solution is characterized by sharp lines except that recorded at 1388 cm^{-1} which shows the mentioned shoulder at 1416 cm^{-1}. This is the characteristic symmetric stretching vibration of the carboxylate, $\nu_s(COO^-)$, which is predicted at 1278 and 1384 cm^{-1} from B3LYP and M06-HF/LanL2DZ calculations, respectively. B3LYP/LanL2DZ calculations underestimates the wavenumber of this mode as was already detected in the case of benzoate [49], but it can be improved using larger basis sets. For instance, a wavenumber of 1347 cm^{-1} is calculated at B3LYP/6-31G* level. The band appearing at about 1420 cm^{-1} in the SERS has been assigned to $\nu_s(COO^-)$ according to the shift predicted by the calculations and shows a shoulder in the red side which becomes stronger at electrode potentials more negative than -0.5 V. These two bands have been assigned to the same $\nu_s(COO^-)$ vibration of molecules adsorbed with different type of coordination as will be discussed in the last Section.

3.2 Vibrational Wavenumber Shifts Due to Molecular Adsorption on the Metal Surface

The adsorption of a molecule on a metallic surface shifts the vibrational wavenumbers, which can thereafter be tuned by the applied potential. Figure 3 shows the experimental differences ($\Delta\nu_{ads,exp}$) between the wavenumbers of the main modes ν(CN), 8a, $\nu_s(COO^-)$, 9a and 1 recorded in the Raman spectrum of the aqueous solution (ν_{sol}) and in the SERS registered at -0.5 V ($\nu_{SERS,-0.5V}$):

$$\Delta\nu_{ads,exp} = \nu_{SERS,-0.5V} - \nu_{sol}$$

The electrode potential of -0.5 V has been selected as a reference to study the surface adsorption and the tuning of the wavenumbers of the adsorbed molecule by the applied potential. This particular voltage is the midpoint of the screened range of potentials and is close to the potential of zero charge (V_{PZC}) of a polycrystalline silver electrode [50,51]. Experimental shifts $\Delta\nu_{ads,exp}$ are compared in Figures 3 and S2 with the respective theoretical predictions ($\Delta\nu_{ads,cal}$) obtained from the M06-HF and B3LYP/LanL2DZ calculated wavenumbers, respectively, for isolated $4CNB^-$ (ν_{4CNB-}) and their complexes with neutral Ag_8^0

silver clusters ($\nu_{(Ag8\text{-}4CNB)\text{-}}$) bonded through the carboxylate $[Ag_8^0\text{-}OOC(4CNB^-)]^{-1}$ or the nitrile $[Ag_8^0\text{-}NC(4CNB^-)]^{-1}$ groups:

$\Delta\nu_{ads,cal} = \nu_{(Ag8\text{-}4CNB\text{-})\text{-}1} - \nu_{4CNB\text{-}}$

The largest experimental shift is shown by the band assigned to the $\nu_s(COO^-)$ mode (+32 cm^{-1}) recorded at 1388 cm^{-1} in the Raman of the solution and at 1420 cm^{-1} in the SERS at -0.5 V, indicating that this group is responsible of the adsorption. The remaining vibrations are much less shifted and in different directions. For instance, the shifts of modes 9a, 1 and 8a amount to +8, +3 and -3 cm^{-1}, respectively.

M06-HF harmonic wavenumbers calculated for both $[Ag_8^0\text{-}OOC(4CNB^-)]^{-1}$ and $[Ag_8^0\text{-}NC(4CNB^-)]^{-1}$ complexes predict an opposite trend for the $\nu_s(COO^-)$ mode (Figure 3). The main result is the large blue-shift of $\nu_s(COO^-)$, +90 cm^{-1}, in the $[Ag_8^0\text{-}OOC(4CNB^-)]^{-1}$ complex, and the small red-shift, -9 cm^{-1}, in the $[Ag_8^0\text{-}NC(4CNB^-)]^{-1}$ system. The remaining vibrations much less much shifted depending on the type of complex. This result agrees with the experimental behaviour, although the calculated shifts are overestimated as we have detected in previous works where it was estimated a factor of ca. 3.5 [21,25]. Another cause of disagreement is the solvation effect, which has not been taken into account in the calculations.

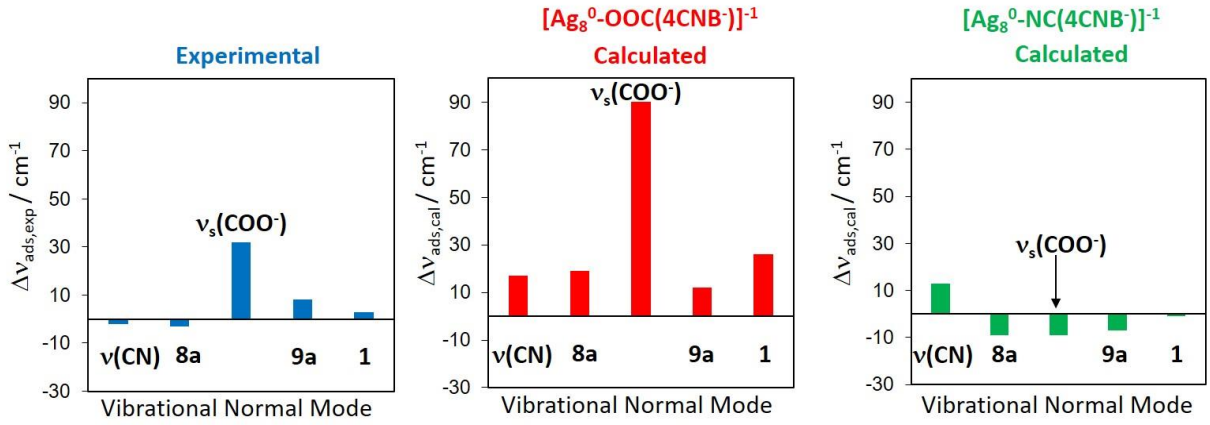

Figure 3. Effect of the adsorption on the experimental wavenumber shifts ($\Delta\nu_{ads,exp} = \nu_{SERS,-0.5V} - \nu_{sol}$, blue) of the most representative normal modes of $4CNB^-$ and on the calculated shifts ($\Delta\nu_{ads,cal} = \nu_{(Ag8\text{-}4CNB)\text{-}1} - \nu_{4CNB\text{-}}$) at M06-HF/LanL2DZ level of theory for $[Ag_8^0\text{-}OOC(4CNB^-)]^{-1}$ (red) and $[Ag_8^0\text{-}NC(4CNB^-)]^{-1}$ (green) complexes.

B3LYP/LanL2DZ results are very similar to M06-HF and do not improve the comparison (Figure S2). M06-HF and B3LYP/LanL2DZ results for the $[Ag_2^0\text{-}NC(4CNB^-)]^{-1}$ complex totally disagree with the experimental behaviour. M06-HF and B3LYP shifts of -9 or -19 cm^{-1} are predicted for the $\nu_s(COO^-)$ vibration and, therefore, this kind of coordination must be discarded.

3.3 Vibrational Wavenumber Shifts Due to the Applied Electrode Potential

Two general trends of the wavenumber shifts are observed in the SERS recorded at different electrode potentials. The wavenumber of some bands as, for instance, those assigned to vibrations 1 or $\nu_s(COO^-)$ remain almost constant at potentials more positive than -0.5 V but are linearly redshifted when the voltage is made more negative. A similar trend, but with much smaller amplitude, is also observed for the wavenumbers of the vibrational modes 9a, ν(CN), ν(C-CN) or ν(C-COO) ring-substituent fundamentals. On the contrary, the 8a mode recorded at ca. 1608 cm^{-1} is almost insensitive to the potential. Summarizing, SERS wavenumbers $4CNB^-$ show a complex and dual behaviour already observed in the case of the simple cyanide anion [21,52] where the wavenumber of the single CN stretching vibration remained almost constant at positive potentials while was redshifted -25 cm^{-1} at negative voltages.

The wavenumbers recorded in the SERS at -0.5 V are considered again as a reference to analyze the effect of the applied potential in tuning the vibrational wavenumbers:

$$\Delta\nu_{V,exp} = \nu_{SERS,V} - \nu_{SERS,-0.5V}$$

Given that the potential controls the surface excess of charge of the electrode, the experimental $\Delta\nu_{V,exp}$ can be compared with the dependence ($\Delta\nu_{qeff,cal}$) of the calculated wavenumbers on the density of charge ($q_{eff} = q/n$) of the linear Ag_n^q silver clusters, which are obtained by subtracting the calculated wavenumbers for charged $[Ag_n^q\text{-}4CNB^-]^{q-1}$ supermolecules and those corresponding to the neutral $[Ag_8^0\text{-}4CNB^-]^{-1}$ species:

$$\Delta\nu_{qeff,cal} = \nu_{(Agn\text{-}4CNB\text{-})q\text{-}1} - \nu_{(Ag8\text{-}4CNB\text{-})\text{-}1}$$

Experimental $\Delta\nu_{V,exp}$ and calculated $\Delta\nu_{qeff,cal}$ using M06-HF and B3LYP functionals are compared in Figures 4 and S3, respectively. The formation of the surface complex causes charge donation from unshared electron pairs of the molecule to vacant orbitals of the metal, making stronger the structure of the molecule due to the non-bonding character of the transferred density of charge. Therefore, molecule-to-metal charge donation is responsible for the blue shifts of the vibrational wavenumbers of $4CNB^-$ upon adsorption and, very especially, of the $\nu_s(COO^-)$ symmetric stretching mode of the carboxylate which is directly involved in the surface bonding. Metal-molecule interaction should be favoured at positive potentials, when molecule and metal have opposite net charges and a larger amount of charge should be transferred, but the complex will get weaker as the potential becomes more negative. This is the reason of the redshifts shown by the SERS bands at negative potentials as was already found in the electrochemical SERS experiments of pyridine [25] or cyanide [21]. But the observed behaviour of the five selected modes shown in Figure 4 is very different.

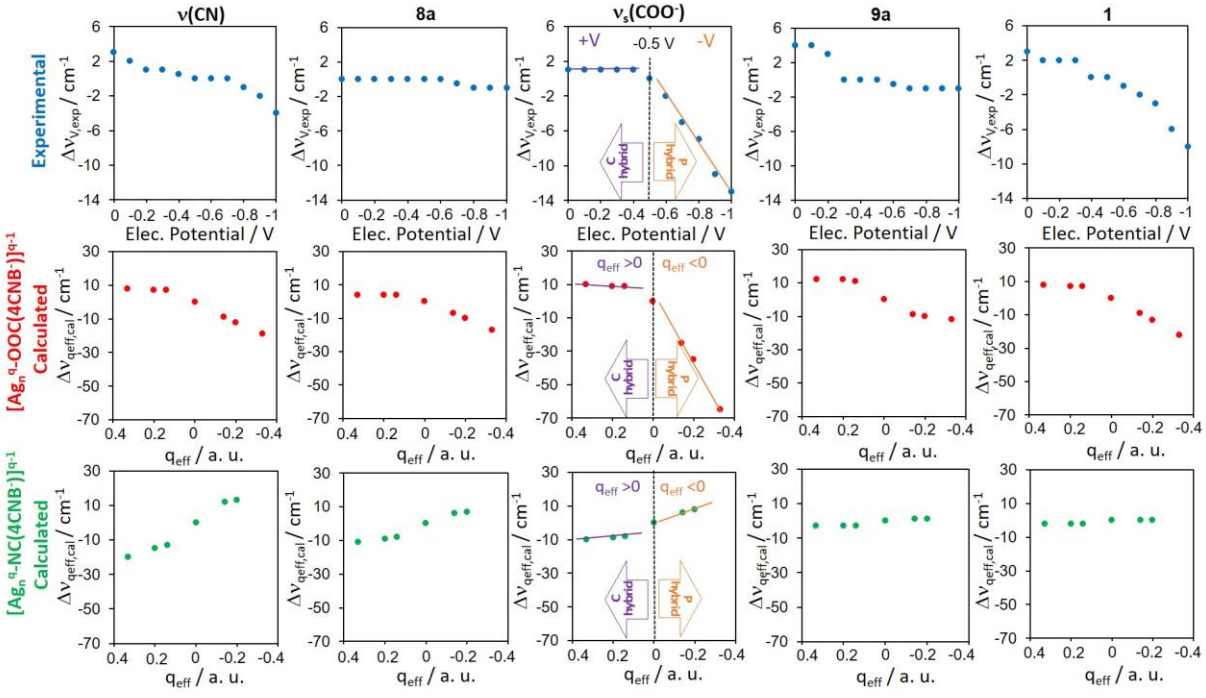

Figure 4. Dependence of the experimental wavenumber shifts of the most representative normal modes of $4CNB^-$ on the electrode potential ($\Delta\nu_{V,exp} = \nu_{SERS,V} - \nu_{SERS,-0.5V}$, blue) and effect of the density of the charge of the Ag_n^q clusters (q_{eff}) on the calculated shifts ($\Delta\nu_{qeff,cal} = \nu_{(Agn\text{-}4CNB)q\text{-}1} - \nu_{(Ag8\text{-}4CNB)\text{-}1}$) at M06-HF/LanL2DZ level of theory for $[Ag_n^q\text{-}OOC(4CNB^-)]^{q-1}$ (red) and $[Ag_n^q\text{-}NC(4CNB^-)]^{q-1}$ (green) complexes.

The wavenumbers of $\nu_s(COO^-)$ and 1 modes remain almost constant at potentials more positive than -0.5 V but are strongly redshifted at negative potentials. The respective tuning amplitudes are -14 and -11 cm^{-1} while the remaining vibrations are much less sensitive to the voltage. Amplitudes for 9a and ν(CN) modes amount to -5 and -7 cm^{-1}, respectively, and the amplitude of the 8a ring-stretching vibration is only -1 cm^{-1}. This last result is different to that observed in a neutral system like pyridine [25] where the 8a;ν_{ring} band showed the largest amplitude of ca. -10 cm^{-1} while the remaining bands were almost linearly shifted in the whole range of potentials. Pyridine is bonded to silver nanoparticles through the electron pair of the nitrogen atom, which is part of the ring and, therefore, the adsorption affects the strength of the aromatic system, and the ring-stretching vibrations should be affected. Opposite, $4CNB^-$ is adsorbed through the carboxylate but this functional group is not involved in the 8a normal mode. The internal coordinates of the carboxylate contribute to mode 1 whose wavenumber is strongly dependent on the kind of benzene substitution [43] as well as on the ionization state of the functional group [49]. This is the reason why $\nu_s(COO^-)$ and 1 modes show the largest dependences on the applied voltage and why non-sensitive fundamentals of para-substituted benzenes, like vibrations 8a and 9a, remain almost unshifted.

The experimental behaviour is qualitatively reproduced by M06-HF calculations carried out for the complex bonded through the carboxylate. M06-HF/LanL2DZ wavenumbers of $[Ag_n^q\text{-}OOC(4CNB^-)]^{q-1}$ remain almost constant at positive q_{eff} but are redshifted when q_{eff} takes negative values. The largest $\Delta\nu_{qeff,cal}$ is predicted for $\nu_s(COO^-)$ (-75 cm^{-1}), while smaller amplitudes are calculated for ν(CN), 1 and 9a vibrations (-27, -30 and -24 cm^{-1}, respectively). 8a mode shows the smallest shift (-21 cm^{-1}) in agreement with the experiment. However, all these amplitudes are overestimated again as it was already observed in the case of pyridine [25] or cyanide [21] where the effect of q_{eff} on the amplitude of the wavenumber shifts was overestimated about 3.5 times with respect to the experimental SERS results.

A totally opposite trend is predicted for the $[Ag_n^q\text{-}NC(4CNB^-)]^{q-1}$ complex bonded to the metal through the cyanide. M06-HF calculated wavenumbers are slightly blue-shifted at negative densities of charge of the clusters as can be seen in Figure 4, where the results for q_{eff}=-0.33 a.u. have been not plotted because the $[Ag_3^{-1}\text{-}NC(4CNB^-)]^{-2}$ complex dissociates. ν(CN) and 8a modes are now blue-shifted +33 cm^{-1} and +18 cm^{-1}, respectively, and very small amplitudes are calculated for 9a and 1 vibrations (+4 and +2 cm^{-1}, respectively), while $\nu_s(COO^-)$ is the only redshifted (-3 cm^{-1}). These predictions totally disagree with the

experiments and, therefore, the existence of a complex where $4CNB^-$ is bonded to silver through the cyanide have to be discarded.

B3LYP/LanL2DZ calculated results summarized in Figure S3 are quite different. $[Ag_3^{-1}\text{-}OOC(4CNB^-)]^{-2}$ complex (q_{eff}=-0.33 a.u.) is almost dissociated at this level, what makes their calculated amplitudes very large. For instance, $\nu_s(COO^-)$ and ν(CN) wavenumbers remain constants at q_{eff}>0 a.u. but are tuned -95 and -138 cm^{-1} at negative densities of charge, respectively. An amplitude of -23 cm^{-1} is predicted for the 8a mode while its experimental wavenumber is almost insensitive to the applied potential. Nevertheless these results better agree with the experiments that those calculated for the respective $[Ag_n^q\text{-}NC(4CNB^-)]^{q-1}$ complex where small redshifts are predicted for all normal modes, around -10 cm^{-1}, except in the case of the $\nu_s(COO^-)$ mode which shows an anomalous sudden jump at q_{eff} = 0 a.u.

As a conclusion, the observed dependence of the SERS wavenumbers on the electrode potential is well reproduced by the calculated results for the $[Ag_n^q\text{-}OOC(4CNB^-)]^{q-1}$ complex at the M06-HF/lanL2DZ level of calculation.

3.4 Dual Electronic Structure of the Surface at Positive and Negative Electrode Potentials

The dual dependence of the SERS wavenumbers at positive and negative electrode potentials is due to existence of two different types of electronic structures of the surface complex. Figures 5a and S4 shows the effect of the effective charge q_{eff} on the M06-HF and B3LYP/LanL2DZ calculated energies of formation ($\Delta E_f = E_{M\text{-}A}\text{-}(E_M+E_A)$) of the two series of metal-adsorbate (M-A) chelating complexes bonded though the carboxylate and the cyanide shown in Figure 1, respectively.

The two series of ΔE_f calculated for $[Ag_n^q\text{-}OOC(4CNB^-)]^{q-1}$ and $[Ag_n^q\text{-}NC(4CNB^-)]^{q-1}$ systems are linearly dependent on q_{eff}, but they show two differentiated branches separated by a gap at q_{eff}=0 a.u. At positive densities of charge both complexes are very stable and are characterized by a small dependence on q_{eff}. The complexes coordinated through the carboxylate group at q_{eff}>0 are much more stable (ca. 2 eV (50 Kcal/mol)) than the corresponding $[Ag_n^q\text{-}NC(4CNB^-)]^{q-1}$. M06-HF energies for the most stable $[Ag_n^q\text{-}OOC(4CNB^-)]^{q-1}$ system range from -5.46 to -4.75 eV (-126.06 and -109.85 Kcal/mol) for q_{eff}=+0.33 and +0.14 a.u., respectively. All these large ΔE_f values are in the order of a chemical bond and, therefore, $4CNB^-$ can be considered as a chemisorbed species (C-hybrid)

strongly bonded to silver surface due to the attractive Coulombic interaction between the positive charge of the electrode and the negative charge of the molecule which is mainly located in the carboxylate. This very stable C-hybrid is almost insensitive to the amount of positive charge of the metal, which explains the observed flat dependences of the SERS wavenumbers (Figure 4) at more positive voltages than -0.5 V and of the calculated ΔE_f (Figure 5a) for complexes with $q_{eff}>0$. Similar conclusion is derived from the calculated metal-molecule R(Ag-O) or R(Ag-N) distances which remain almost constant along this range of positive metal charges (Figures 5b and S4b).

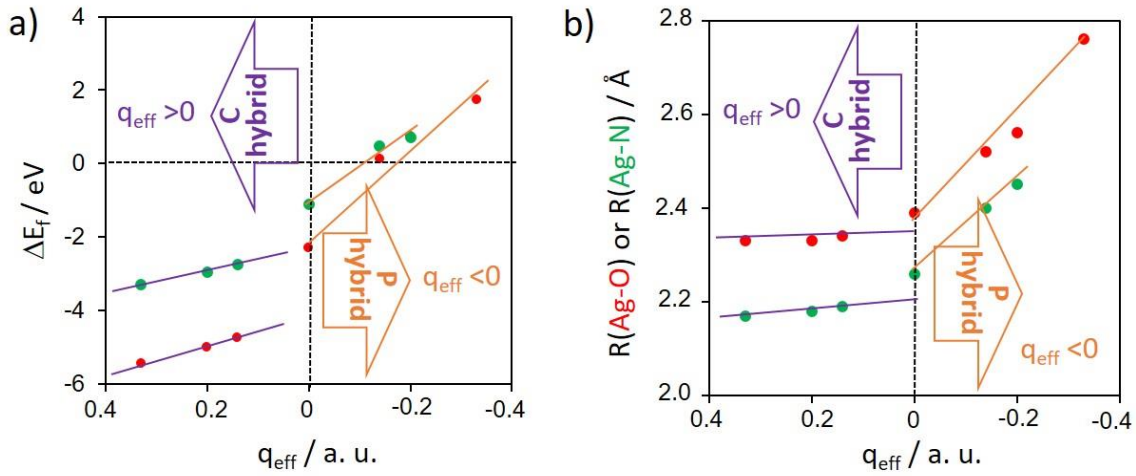

Figure 5. Effect of the effective charge q_{eff} of the Ag_n^q clusters on the calculated a) M06-HF/LanL2DZ energies of formation ΔE_f (eV) and b) bond lenghts between the terminal silver atom of the metallic cluster and the oxygen or the nitrogen of $[Ag_n^q\text{-}OOC(4CNB^-)]^{q-1}$ (red) and $[Ag_n^q\text{-}NC(4CNB^-)]^{q-1}$ (green) surface complexes, respectively.

Conversely, M06-HF and B3LYP results for $q_{eff}<0$ are qualitative different due to strong electrostatic repulsion between negative charges. The systems are now much less stable than in the previous case what implies that the metal-molecule bond is significantly weaker and, therefore, these complexes can be considered as physisorbed systems (P-hybrid). Positive values of ΔE_f are calculated for these P-hybrids which, however, remain stable due to the existence of a local minimum in the potential energy surface [27]. M06-HF energies of $[Ag_n^q\text{-}OOC(4CNB^-)]^{q-1}$ complexes with $q_{eff}<0$ are much smaller than in the previous case and show a strong dependence on q_{eff}. Their ΔE_f values range from +0.11 to +1.73 eV (+2.75 and +39.88 Kcal/mol) for the respective systems with q_{eff}=-0.14 and -0.33 a.u. B3LYP calculations predict very similar results and trend (Figure S4), but the repulsion is too large at

q_{eff}=-0.33 a.u. and the $[Ag_3^{-1}\text{-}NC(4CNB^-)]^{-2}$ complex dissociates when the geometry optimization is carried out.

The main qualitative difference between C- and P-hybrids is the slope of the respective ΔE_f vs. q_{eff} plots. The density of charge of the clusters is much more effective in tuning ΔE_f in the repulsive complex ($q_{eff}<0$) than in the attractive one ($q_{eff}>0$) (Figures 5a and S4a). This points out that the electronic structure of the surface complex is very polarizable at electrode potentials more negative than V_{PZC}. The increasing metal-molecule repulsion is responsible for the large tunning amplitudes of the SERS wavenumbers at negative voltages which gradually reduce the large blue-shift of the wavenumbers induced by the adsorption. The calculated metal-adsorbate distances for the P-hybrid at negative q_{eff} (Figures 5b and S4b) also show a larger dependence on the density of charge of the metal clusters.

The charges of the two moieties, $4CNB^-$ and Ag_n^q clusters, undergo redistribution when the surface complex is formed. The metal-molecule bond is formed from charge donation from the lone electron pairs of the carboxylate to vacant orbitals of the metal accompanied by backdonation from the metal to the molecule, giving a net injection of charge from $4CNB^-$ to Ag_n^q ($\Delta q_{4CNB^-\rightarrow Ag}$) in the overall range of electrode potentials. The dependence of the calculated injected Mulliken´s charges $\Delta q_{4CNB^-\rightarrow Ag}$ on q_{eff} is shown in Figure S5 and confirms the expected behavior. A net negative charge is transferred from the molecule to the metal at any q_{eff}. The calculated $\Delta q_{4CNB^-\rightarrow Ag}$ values are sensitive to the functional (M06-HF/LanL2DZ and B3LYP/LanL2DZ) and the type of coordination ($[Ag_n^q\text{-}OOC(4CNB^-)]^{q-1}$ and $[Ag_n^q\text{-}NC(4CNB^-)]^{q-1}$) but all of them show again the dual behavior already discussed and corresponding to the C- and P-hybrids.

Summarizing, chemisorbed and physisorbed electronic structures are selected by the sign of q_{eff} and a sudden transition between them is expected at q_{eff}=0 a.u. which corresponds to the complexes formed with neutral silver clusters $[Ag_8^0\text{-}4CNB^-]^-$ being related to the metal-molecule interface at the potential of zero charge of the electrode.

3.5 Dependence of the Type of Coordination on the sign of the Surface Excess of Charge of the Metal Nanostructure

Theoretical calculations also predict that the sign of the density of charge of the surface can also modify the type of preferred coordination between the carboxylate and the silver surface of the $[Ag_n^q\text{-}OOC(4CNB^-)]^{q-1}$ complexes. Carboxylate can be bonded to silver with bidentate

chelating coordination such as the C_{2v} systems drawn in Figure 1 (CHE-C_{2v}), but bidentate bridging (BRI-C_{2v}) or monodentate (MON-C_s) complexes could be also formed. Geometry optimizations of these three types of coordination with linear (L) or triangular (T) Ag_3^q clusters with the largest densities of charge (q_{eff}=+0.33 or -0.33 a.u.) have been performed. M06-HF and B3LYP/LanL2DZ calculations provide similar results which have been summarized in Figures 6 and S6, respectively. Both levels of calculation predict that the bridge coordination BRI-T-C_{2v} is preferred at positive q_{eff} but becomes the most unstable at negative densities of charge being replaced by the monodentate MON-L-C_s. The attractive character of the C-hybrid favours the bonding of each negative oxygen of the carboxylate to one positive silver atoms of the surface. Optimized geometries of monodentate complexes cannot be obtained for neutral or positively charged Ag_n^q complexes giving that they converge to the respective chelating structures.

The two Ag-O links of the bridging complex weaken as the positive charge of the surface decreases. The electrostatic repulsion existing at q_{eff}<0 a.u. is able to open the bridge and producing monodentate structures which become the most stable. Anyway, M06-HF ΔE_f energies of the chelating structures CHE-L-C_{2v} shown in Figure 1 are only 9.26 and 5.20 Kcal/mol (6.90 and 15.10 Kcal/mol from B3LYP) less stables than the preferred bridge (q_{eff}>0) and monodentate (q_{eff}<0) coordinations of the C- and P-hybrids, respectively, what points to the probable coexistence of different types of surface bonding in real electrodes and to discard monodentate complexes at electrode potentials more positive than V_{PZC}. Monodentate complexes are more stable than the corresponding $[Ag_n^{-1}\text{-}OOC(4CNB^-)]^{-2}$ chelating complexes at q_{eff}<0 a.u., with ΔE_f energies -1.22, -2.32 and -5.20 Kcal/mol lower than those of the corresponding chelating complexes with n=7, 5 and 3, respectively (See Figure S7).

q_{eff} = +0.33 a.u.	CHE-L-C_{2v}	BRI-T-C_{2v}	CHE-T-C_{2v}	MON-L-C_s	MON-T-C_s
$[Ag_3^{+1}$-OOC(4CNB$^-$)$]^0$ Ag_n^q clusters: q=+1 a.u. n=3	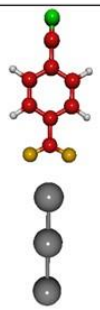	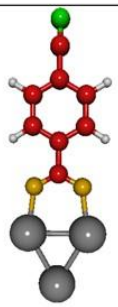	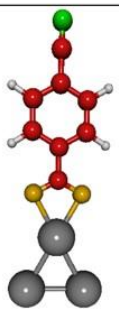	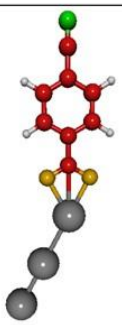	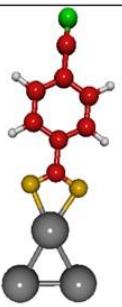
Symmetry	C_{2v}	C_{2v}	C_{2v}	C_s	C_s
ΔE_f (Kcal/mol)	-126.06	-135.32	-118.91	-125.81	-118.87
Relative ΔE_f (Kcal/mol)	0.0	-9.26	+7.15	+0.19	+7.19
$\nu_s(COO^-)$ (cm^{-1})	1484	1467	1481	1484	1473

q_{eff} = -0.33 a.u.	CHE-L-C_{2v}	BRI-T-C_{2v}	CHE-T-C_{2v}	MON-L-C_s	MON-T-C_s
$[Ag_3^{-1}$-OOC(4CNB$^-$)$]^{-2}$ Ag_n^q clusters: q=-1 a.u. n=3	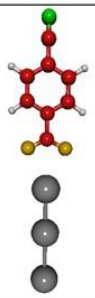	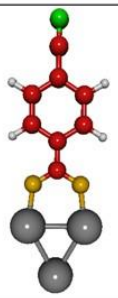	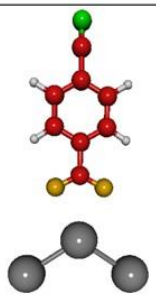	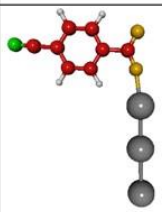	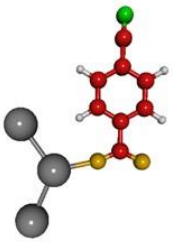
Symmetry	C_{2v}	C_{2v}	C_{2v}	C_s	C_s
ΔE_f (Kcal/mol)	+39.88	+51.37	+50.91	+34.68	+41.59
Relative ΔE_f (Kcal/mol)	0.0	+11.49	+11.03	-5.20	+1.71
$\nu_s(COO^-)$ (cm^{-1})	1409	1424	1413	1384	1388

Figure 6. M06-HF/LanL2DZ energies of formation (ΔE_f) and $\nu_s(COO^-)$ wavenumbers of $[Ag_3^q$-OOC(4CNB$^-$)$]^{q-1}$ complexes with bidentate chelating (CHE), bidentate bridging (BRI) or monodentate (MON) coordination of 4CNB$^-$ bonded to linear (L) or triangular (T) Ag_3^{+1} and Ag_3^{-1} clusters (q_{eff} =+0.33 and -0.33 a.u.) through the carboxylate.

This result could explain the complex behaviour of the $\nu_s(COO^-)$ SERS band which shows several components in the spectra recorded at negative potentials. The weak and broad shoulder that can be seen in the red side of the band at positive potentials turns into one or two resolved peaks at potentials more negative than -0.5 V. This could be due to the increase of monodentate surface coverage given that their calculated $\nu_s(COO^-)$ wavenumbers are 20-40 cm^{-1} lower than those of the corresponding bidentate complexes (Figures 6, S6 and S7).

Conclusions

The voltage (E_V) dependence of the SERS wavenumbers of 4-cyanobenzoate ($4CNB^-$) adsorbed on a charged nanostructured silver electrode has been analysed with the support of DFT calculations modelling the metal-molecule surface complex through linear Ag_n^q silver clusters with different densities of charge ($q_{eff}=q/n$). The adsorption has a very specific impact on the wavenumber of the symmetric stretching mode of the carboxylate $\nu_s(COO^-)$. The subsequent application of electric potentials affects the SERS wavenumbers of the main normal modes in a complex way. Some of them remain almost insensitive while the wavenumbers of $\nu_s(COO^-)$ and $1;\nu_{ring}$ vibrations show a dual behaviour at positive or negative potentials with respect to -0.5 V. The electrode potential is unable to shift these two bands when E_V>-0.5 V while a strong dependence of the respective wavenumbers is observed at more negative values.

M06-HF and B3LYP/LanL2DZ calculations on the relative stability and the vibrational wavenumbers of charged metal-molecule complexes bonded through the carboxylate or the nitrile groups have turned out to be very useful in order to account for the experimental results. As a conclusion, $4CNB^-$ is adsorbed on the silver electrode through the carboxylate in all the range of studied potentials and the coordination through the nitrile is discarded. Moreover, the dual dependence of the SERS wavenumbers on the electrode potential is due to the existence of two kinds of metal-molecule complexes, which are selected at more positive (C-hybrid) or negative (P-hybrid) voltages than the potential of zero charge of the electrode. A very stable chemisorbed C-hybrid exists at positive potentials due to the strong attractive interaction between the opposite net charges of the molecular anion and the positive surface. Its electronic structure is so robust that the voltage is almost unable to modify the SERS wavenumbers. On the contrary, repulsive interaction between the negative charges of the molecule and the metal occurs at electrode potentials more negative than V_{PZC} giving a weaker physisorbed P-hybrid whose electronic structure and stability is very dependent on the surface excess of charge of the electrode, i.e., on the applied potential. The effect of E_V on the SERS wavenumbers reflects the tuning of this very polarizable electronic structure of the physisorbed species.

Physisorbed and chemisorbed molecules such as $4CNB^-$ do not produce evident changes in the geometry or the molecular properties of the surface complex what makes very difficult to experimentally discriminate the presence of one or another species. The existence of this dual electronic structure was theoretically predicted by studying the effect of the electrode potential on the energies of the metal-molecule excited charge-transfer states of isonicotinate

anion bonded to charged metal clusters [27]. This conclusion was confirmed, for the first time, by studying the dependence of the SERS wavenumbers of the simple diatomic cyanide anion [21,52]. This work shows how the electrode potential selects the type of adsorption, physical or chemical, of a rather complex polyatomic molecule. Both kind of surface complex are sharply characterized and show a differentiated electronic structure, which determine all the physicochemical properties of the surface complex in both the ground and excited electronic states. This finding can be very useful in order to understand the complex behaviour of metal interfaces containing adsorbed organic molecules which are the key part of classical electrodics as well as of novel devices based on molecular electronics.

CRediT authorship contributions.

Samuel Valdivia: DFT calculations

Francisco José Avila: DFT calculations

Juan Carlos Otero: Supervision, Writing-review, Funding acquisition.

Isabel López-Tocón: Conceptualization, Investigation, Experimental SERS records, DFT calculations, Writing-original draft, Writing-review & editing.

Conflicts of interest

The authors declare that they have no known competing financial interest or personal relationships that could have appeared to influence the work reported in this paper.

Acknowledgements

This research has been supported by Junta de Andalucía/FEDER (UMA18-FEDERJA-049 and P18-RT-4592). The authors thanks to the Supercomputing and Bioinnovation Center (University of Málaga) for computational resources and Rafael Larrosa for technical support.

Supplementary Material

Supplementary data available at…

References

[1] R. Aroca, Surface-Enhanced Vibrational Spectroscopy, John Wiley & Sons Ltd., Chichester, UK, 2006.

[2] L. Furini, C. Constantino, S. Sanchez-Cortes, J.C. Otero, I. López-Tocón, Adsorption of carbendazim pesticide on plasmonic nanoparticles studies by surface-enhanced Raman

scattering, J. Coll. Interface Sci. 465 (2016) 183-189. https://doi.org/10.1016/j.jcis.2015.11.045.

[3] K. Kneipp, H. Kneipp, I. Itzkan, R.R. Dasari, M.S. Feld, Surface-enhanced Raman Scattering (SERS)-A tool for single molecule detection in solution. In Single-Molecule Detection in Solution: Methods and Applications, J. Enderlein, R.A. Keller, C. Zander. Eds., VCH-Wiley; Weinheim, Germany, 2001.

[4] I. López-Tocón, J.C. Otero, J.F. Arenas, J.V. García-Ramos, S. Sánchez-Cortés, Trace Detection of Triphenylene by Surface Enhanced Raman Spectroscopy Using Functionalized Silver Nanoparticles with Bis-Acridinium Lucigenine, Langmuir 26 (2010) 6977-6981. https://doi.org/10.1021/la904204s.

[5] T.M. Devine, Use of Surface-Enhanced Raman Spectroscopy in Studies of Electrode-Electrolyte Interfaces. In Electrochemical and Optical Techniques for the Study and Monitoring of Metallic Corrosion, Springer Science and Business Media LLC, Berlin, Germany, 1991, pp.389.

[6] C. Shi, W. Zhang, R.L. Birke, J.R. Lombardi, SERS investigation of the adsorption and electroreduction of 4-cyanopyridine on a silver electrode, J. Electroanal. Chem. 423 (1997) 67-81. https://doi.org/10.1016/S0022-0728(96)04810-3.

[7] E. Lee, S.S. Yi, M.S. Kim, K.Kim, Adsorption of aromatic nitriles on silver investigated by Raman spectroscopy, J. Mol. Struct. 298 (1993) 47-54. https://doi.org/10.1016/0022-2860(93)80206-B.

[8] M.L. Patterson, M.J. Weaver, Adsorption and oxidation of ethylene at gold electrodes as examined by surface-enhanced Raman spectroscopy, J. Phys. Chem. 89 (1985) 1331-1334. https://doi.org/10.1021/j100254a003.

[9] T.H. Joo, K. Kim, M.S. Kim, Surface-Enhanced Raman Scattering (SERS) of 1-propanethiol in silver sol, J. Phys. Chem. 90 (1986) 5816-5819. https://doi.org/10.1021/j100280a069.

[10] M. Takahashi, H. Furukawa, M. Fujita, M. Ito, Surface-enhanced Raman spectra of phthalazine: anion-induced reorientation on a silver electrode, J. Phys. Chem. 1987, 91, 5940-5943. https://doi.org/10.1021/j100307a025.

[11] I. López-Tocón, S. Valdivia, J. Soto, J.C. Otero, F. Muniz-Miranda, M.C. Menziani, M. Muniz-Miranda, 2019. A DFT approach to the Surface-Enhanced Raman Scattering of 4-Cyanopyridine adsorbed on silver nanoparticles. Nanomaterials. 9, 1211. https://doi.org/10.3390/nano9091211.

[12] S.S. Yi, K. Kim, M.S. Kim, Investigation of adsorption and decomposition of 4-(methylthio)benzonitrile on a silver surface by Raman spectroscopy, J. Raman Spectrosc. 24 (1993) 213-219. https://doi.org/10.1002/jrs.1250240406.

[13] S.H. Kim, S.J. Ahn, K. Kim, Vibrational Spectroscopic Study of 4-Cyanobenzoic Acid Adsorbed on Silver, J. Phys. Chem. 100 (1996) 7174-7180. https://doi.org/10.1021/jp953309r.

[14] S.W. Han, H.S. Han, K. Kim, Infrared and Raman spectra of 4-cyanobenzoic acid on powdered silver, Vibr. Spectrosc. 21 (1999) 133-142. https://doi.org/10.1016/S0924-2031(99)00066-1.

[15] D.A. Perry, J.S. Cordova, W.D. Spencer, L.G. Smith, A.S. Biris, SERS, SEIRA, TPD and DFT Study of Cyanobenzoic Acid Isomer Film Growth on Silver Nanostructured Films and Powder, J. Phys. Chem. C 114 (2010) 14953-14961. https://doi.org/10.1021/jp104256h.

[16] R. Holz, The adsorption of nitrobenzene and benzonitrile on silver electrodes as studied with surface enhanced Raman spectroscopy sers, Electrochim Acta 36 (1991) 1523-1526. https://doi.org/10.1016/0013-4686(91)85343-6.

[17] X. Gao, J.P. Davies, M.J. Weaver, Test of surface selection rules for surface-enhanced Raman scattering: the orientation of adsorbed benzene and monosubstituted benzenes on gold, J. Phys. Chem. 94 (1990) 6858-6864. https://doi.org/10.1021/j100380a059.

[18] A. Chen, J. Richer, S.G. Roscoe, J. Lipkowski, Electrochemical and Fourier Transform Infrared Spectroscopy Studies of Benzonitrile Adsorption at the Au(111) Electrode, Langmuir 13 (1997) 4737-4747. https://doi.org/10.1021/la9701586.

[19] M. R. Albert, J.T. Yates, The surface Scientist's Guide to Organometallic Chemistry, American Chemical Society, Washington DC (USA), 1987. https://doi.org/10.1002/ange.19881000432.

[20] H.A. Chun, S.S. Yi, M.S. Kim, K. Kim, Adsorption and reaction of 4-methoxycinnamonitrile on a silver surface: A surface-enhanced Raman spectroscopic study, J. Raman Spectrosc. 21 (1990) 743-749. https://doi.org/10.1002/jrs.1250211107.

[21] S. Valdivia, D. Aranda, F.J. Avila Ferrer, J. Soto, I. López-Tocón, J.C. Otero, Proving the Dual Electronic Structure of Charged Metal-Molecule Interfaces: Surface-Enhanced Raman Scattering of Cyanide Adsorbed on a Nanostructured Silver Electrode, J. Phys. Chem. C 124 (2020) 32, 17632–17639. https://doi.org/10.1021/acs.jpcc.0c04130.

[22] H.S. Han, C.H. Kim, K. Kim, Diffuse Reflectance Infrared Spectra of 4-Nitrobenzoic Acid and 4-Cyanobenzoic Acid Self-Assembled on Fine Silver Particles, Appl. Spectrosc. 52 (1998) 1047-1052. https://doi.org/10.1366/0003702981944931

[23] T. Wadayama, O. Suzuki, Y. Suzuki, A. Hatta, Infrared absorption enhancement of p-cyanobenzoic acid on silver island films deposited on oxidized and hydrogen-terminated Si(100) surfaces, Appl. Phys. A: Materials Science and Processsing 64 (1997) 501-506.

[24] P. Johansson, Illustrative direct ab intio calculations of surface Raman spectra, Phys. Chem. Chem. Phys. 2005, 7, 475-482. https://doi.org/10.1039/B415535A.

[25] D. Aranda, S. Valdivia, J. Soto, I. López-Tocón, F.J. Avila, J.C. Otero, 2019. Theoretical approaches for Modelling the effect of the electrode Potential in the SERS Vibrational Wavenumber of Pyridine Adsorbed on a Charged Silver Surface. Front. Chem. **7**, 423. https://doi.org/10.3389/fchem.2019.00423.

[26] J. Román-Pérez, I. López-Tocón, J.L. Castro, J.F. Arenas, J. Soto, J.C. Otero, The electronic structure of metal-molecule hybrids in charged interfaces: surface-enhanced Raman selection rules derived from plasmo-like resonances, Phys. Chem. Chem. Phys. 17 (2015) 2326-2329. https://doi.org/10.1039/C4CP04724A.

[27] J. Román-Pérez, S.P. Centeno, M.R. López-Ramírez, J.F. Arenas, J. Soto, I. López-Tocón, J.C. Otero, On the dual character of charged metal-molecules hybrids and the opposite behaviour of the forward and reverse CT processes, Phys. Chem. Chem. Phys. 16 (2014) 22958-22961. https://doi.org/10.1039/C4CP03984J.

[28] M.J. Frisch, G.W. Trucks, H.B. Schlegel, G.E. Scuseria, M.A. Robb, J.R. Cheeseman, G. Scalmani, V. Barone, G.A. Petersson, H. Nakatsuji, et al. Gaussian 09, Revision A.02, Gaussian, Inc. Wallingford, UK, 2010.

[29] A.D. Becke, Density-functional thermochemistry. III. The role of exact exchange, J. Chem. Phys. 98 (1993) 5648-5653. https://doi.org/10.1063/1.464913.

[30] P.J Stephens, F.J. Devlin, C.F. Chabalowski, M.J. Frisch, Ab initio calculation of vibrational absorption and circular dichroism spectra using density functional force fields, J. Phys. Chem. 98 (1994) 11623-11627. https://doi.org/10.1021/j100096a001.

[31] Y. Zhao, D.G. Truhlar, Density functional for spectroscopy: no long-range self-interaction error, good erformance for Rydberg and charge-transfer states, and better performance on average than B3LYP for ground states, J. Phys. Chem. A 110 (2006) 13126-13130. https://doi.org/10.1021/jp066479k.

[32] P.J. Hay, W.R. Wadt, Ab initio effective core potentials for molecular calculations. Potentials for the transition metal atoms Sc to Hg, J. Chem. Phys. 82 (1985) 270-283. https://doi.org/10.1063/1.448799.

[33] P.J. Hay, W.R. Wadt, Ab initio effective core potentials for molecular calculations. Potentials for main group elements Na to Bi, J. Chem. Phys. 82 (1985) 284-298. https://doi.org/10.1063/1.448800.

[34] P.J. Hay, W.R. Wadt, Ab initio effective core potentials for molecular calculations. Potentials for K to Au including the outermost core orbitals, J. Chem. Phys. 82 (1985) 299-310. https://doi.org/10.1063/1.448975.

[35] F.J. Avila, D. Fernández, J.F. Arenas, J.C. Otero, J. Soto, Modelling the effect of the electrode potential on the metal-adsorbate surface states: relevant states in the charge transfer mechanism of SERS, Chem. Commun. 47 (2011) 4210-4212. https://doi.org/10.1039/C0CC05313A.

[36] T. Higashi, K. Osaki, Structure of p-cyanobenzoic acid, Acta Cryst. B37 (1981) 777-779. https://doi.org/10.1107/S0567740881004305.

[37] D. Britton, p-Fluorebenzonitrile, Acta Cryst. B33 (1977) 3926-3928. https://doi.org/10.1107/S0567740877012473.

[38] G. Fauvet, M. Massaux, R. Chevalier, Etude de la forme cristalline du benzonitrile à 198 K., Acta Cryst. B34 (1978) 1376-1378. https://doi.org/10.1107/S0567740878005658.

[39] T. Higashi, K. Osaki, p-Nitrobenzonitrile, Acta Cryst. B33 (1977) 2337-2339. https://doi.org/10.1107/S0567740877008425.

[40] T. Higashi, K. Osaki, p-Cyanophenol, Acta Cryst. B33 (1977) 607-609. https://doi.org/10.1107/S0567740877004269.

[41] V. Arjunan, T. Rani, L. Varalakshmy, S. Mohan, F. Tedlamelekot, DFT and ab initio quantum chemical studies on p-cyanobenzoic acid, Spectrochim, Acta A Mol. Biomol. Spectrosc. 78 (2011) 1449-1454. https://doi.org/10.1016/j.saa.2011.01.026.

[42] G. Schaftenaar, J.H. Noordik, Molden: A pre- and post- processing program for molecular and electronic structures, J. Comput.-Aided Mol. Design 14 (2000) 123-134. https://doi.org/10.1023/A:1008193805436.

[43] G. Varsanyi, Vibrational spectra of Benzene Derivatives, Academic Press, New York, NY, USA, 1969.

[44] C.S. Allen, R.P. van Duyne, Orientational specificity of Raman scattering from molecules adsorbed on silver electrodes, Chem. Phys. Lett. 63 (1979) 455-459. https://doi.org/10.1016/0009-2614(79)80688-0.

[45] H. Furukawa, M. Takahashi, M. Ito, A surface-enhanced Raman study of the electrochemical reduction of 4-cyanopyridine, Chem. Phys. Lett. 132 (1986) 498-501. https://doi.org/10.1016/0009-2614(86)87111-1.

[46] J.F. Arenas, M.A. Montañez, J.C. Otero, J.I. Marcos, Surface enhanced Raman spectra of 2-cyanopyridine and picolinamide, J. Mol. Struct. 293 (1993) 341-344. https://doi.org/10.1016/0022-2860(93)80081-6.

[47] J.A. Creighton. The selection rules for surface-enhanced Raman spectroscopy. In Spectroscopy of Surfaces, R.J.H. Clark, R.E. Hester, Eds. Wiley, Chichester, UK, 1988.

[48] A. Otto, M. Fumata, Electronic Mechanism of SERS. In Surface-Enhanced Raman Scattering, Topics in Applied Physics, K. Kneipp, M. Moskovits, H. Kneipp, Eds.; Springer, Berlin, Germany, 2006 pp-147.

[49] M.R. Lopez-Ramirez, C. Ruano, J.L. Castro, J.F. Arenas, J. Soto, J.C. Otero, Surface-Enhanced Raman Scattering of Benzoate Anion Adsorbed on Silver Nanoclusters: Evidence of the Transient Formation of the Radical Dianion, J. Phys. Chem. C 114 (2010) 17, 7666–7672. https://doi.org/10.1021/jp911865w.

[50] X. Y. Chen, A. Otto, Electronic effects in SERS by liquid water, J. Raman Spectrosc. 36 (2005) 736-747. https://doi.org/10.1002/jrs.1335.

[51] J.T. Hupp, D. Larkin, M.J. Weaver, Specific adsorption of halide and pseudohalide ions at electrochemically roughened versus smooth silver-aqueous interfaces, Surf. Sci. 125 (1983) 429-451. https://doi.org/10.1016/0039-6028(83)90576-9.

[52] J. Billman, A. Otto, Charge transfer between adsorbed cyanide and silver probed by SERS, Surf. Sci. 138 (1984) 1-25. https://doi.org/10.1016/0039-6028(84)90491-6.